

## On the molecular origin of supercapacitance in nanoporous carbon electrodes

C. Merlet<sup>1,2</sup>, B. Rotenberg<sup>1,2</sup>, P.A. Madden<sup>3</sup>, P.-L.

Taberna<sup>2,4</sup>, P. Simon<sup>2,4,5</sup>, Y. Gogotsi<sup>6</sup>, and M. Salanne<sup>1,2,\*</sup>

<sup>1</sup> *UPMC Université Paris 06, CNRS, ESPCI,*

*UMR 7195, PECSA, F-75005 Paris, France*

<sup>2</sup> *Réseau National sur le Stockage Electrochimique de l'Energie (RS2E), FR CNRS n° 3104*

<sup>3</sup> *Department of Materials, University of Oxford, Parks Road, Oxford OX1 3PH, UK*

<sup>4</sup> *Université Paul Sabatier, CIRIMAT,*

*UMR-CNRS 5085, 31062 Toulouse Cedex 4, France*

<sup>5</sup> *Institut Universitaire de France, 103 Boulevard Saint Michel, 75005 Paris, France*

<sup>6</sup> *Department of Materials Science & Engineering,*

*Drexel University, 3141 Chestnut Street,*

*Philadelphia, Pennsylvania 19104, USA and*

*\* e-mail: mathieu.salanne@upmc.fr*

## Simulation boxes details

Carbon type	$T_{\text{synthesis}}$ (°C)	$L_x=L_y$ (Å)	$L_z$ (Å)	Number of atoms for one electrode
CDC-1200	1200	43.68	186.36	3649
CDC-950	950	43.56	186.36	3276

TABLE I: Details of the simulation boxes for the different carbon types. For all the simulations, the box contains 600 ion pairs.  $T_{\text{synthesis}}$  is the temperature at which the synthesis would be carried out to obtain experimentally a carbon with a similar structure.<sup>1</sup>

For both carbon types, two simulation boxes were built: the first where the positions of the atoms in the left electrode are translated (along the  $z$  direction) to give the positions of the atoms in the right electrode, the second where the positions of the atoms in the right electrode are the symmetrical of the positions of the atoms in the left electrode with respect to the  $(xy)$  plane, translated (along the  $z$  direction). These setups are denominated “antisymmetrical” and “symmetrical” respectively. The statistical results in the main text are given as an average of both setups.

### Determination of an appropriate potential for the production runs

When going from the constant charge equilibration runs to the constant potential production runs, it is necessary to choose an appropriate potential difference. A solution is to calculate the Poisson potential across the cell for the constant charge simulations and apply the potential difference obtained in the constant potential runs. The Poisson potential is calculated from:

$$\begin{aligned}\Psi(z) &= \Psi_q(z) \\ &= \Psi_q(z_0) - \frac{1}{\varepsilon_0} \int_{z_0}^z dz' \int_{z_0}^{z'} dz'' \rho_q(z''),\end{aligned}\quad (1)$$

where  $z_0$  corresponds to the lowest value in the  $z$  direction,  $\Psi_q(z_0) = 0.0$  and  $\rho_q(z)$  is the charge density across the cell, which includes the contributions from the electrode atoms as well as from the charges on the sites of the ionic liquid molecules. The profile obtained for the CDC-1200 carbon is given in figure 1. The potential drop of 1.0 V obtained is applied in the constant potential production runs for this carbon type. The potential difference calculated in the same way for the CDC-950 carbon is 0.75 V. For the two carbon types, the potential difference calculated by this method is the same for the “symmetrical” and “antisymmetrical” cells.

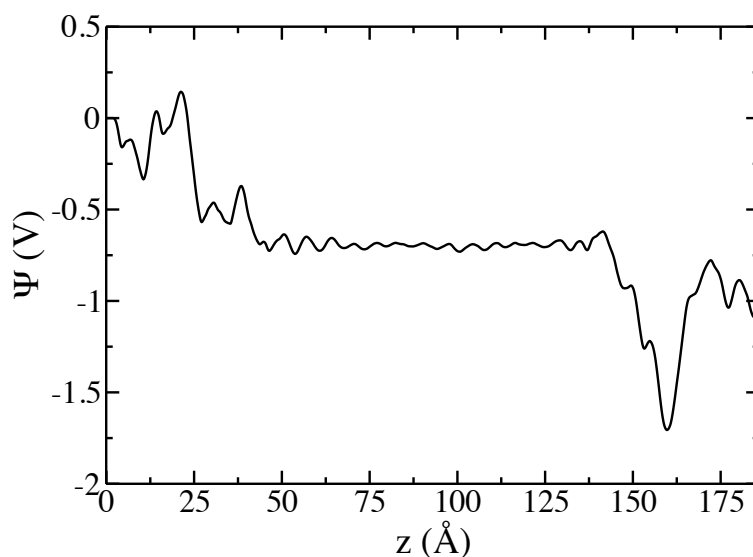


FIG. 1: Poisson potential for the CDC-1200 carbon calculated from the constant charge equilibration. From this plot, we can determine a potential difference of 1.0 V between the positive and negative electrode, this potential difference is thus the one used in the constant potential production runs.

# Coordination numbers along the $z$ direction

To calculate the coordination numbers along the  $z$  axis, the cell is divided into several bins in this direction. The coordination number in a given bin is then obtained by averaging the number of counterions for each ion in this bin. A counterion is counted as a neighbour if the distance between his center of mass and the considered ion center of mass is smaller than the one corresponding to the first minimum of the radial distribution function in the bulk liquid.

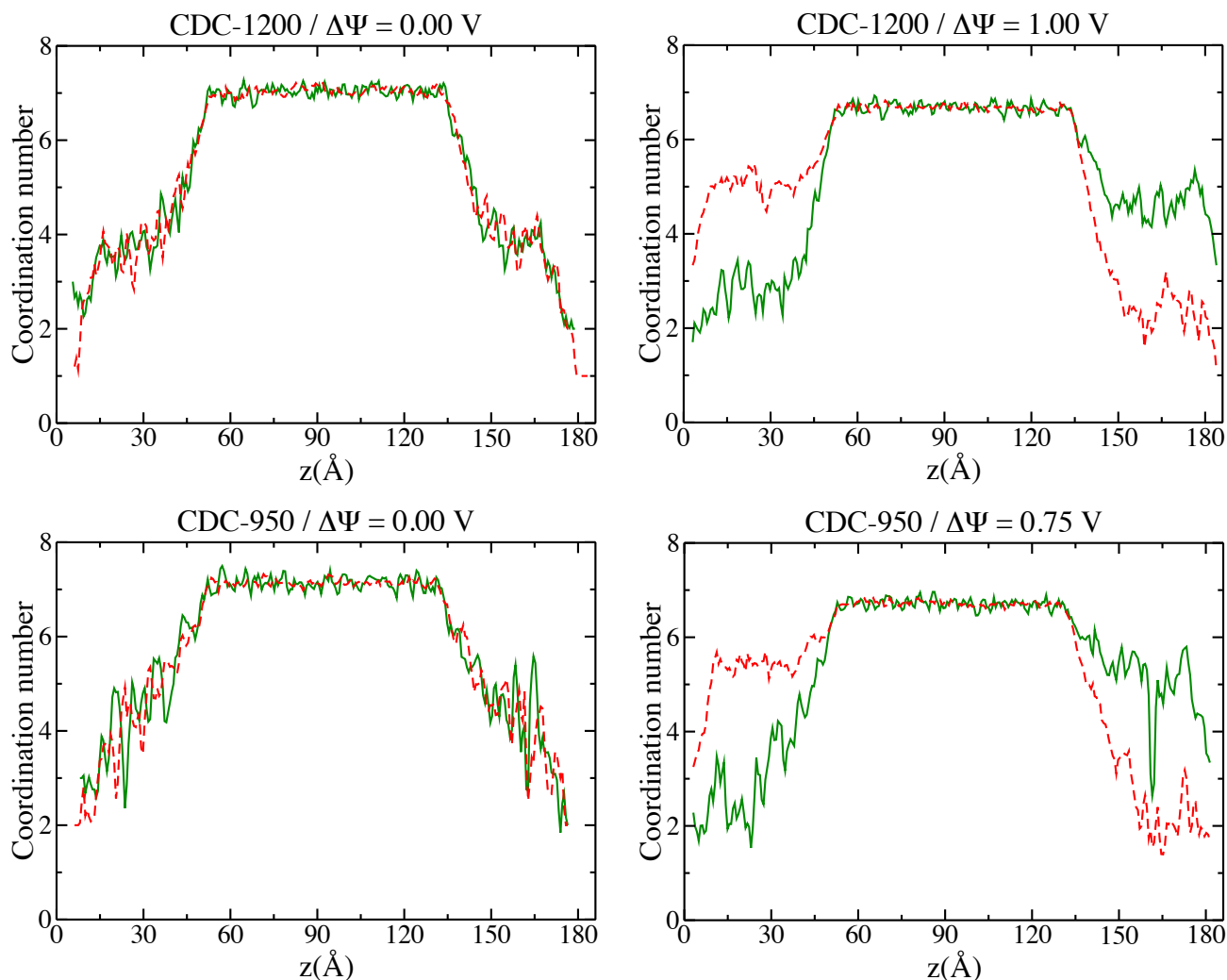


FIG. 2: Coordination numbers along the  $z$  direction for the two carbon types and for the two potential differences applied. Green color (solid line) stands for coordinated cations around anions, red color (dashed line) corresponds to coordinated anions around cations.

### Definition of the accessible surface area and ionic density profiles

The accessible surface area is defined as the surface between the accessible volume and the excluded volume. To calculate the accessible surface area, one has to choose a probe sphere which determines the minimum distance allowed between ions and wall atoms. Here, we take argon as a probe sphere to be able to compare the results with experiments. We also did the analysis with nitrogen as a probe sphere, which gave equivalent conclusions. The indicator function  $\chi(\mathbf{r}) = 1$  if accessible, 0 otherwise, defining the accessible volume is estimated on a grid. The accessible volume is then given by

$$V_{acc} = \int \chi(\mathbf{r}) \, d\mathbf{r} \quad (2)$$

The accessible surface is the region where the gradient  $\|\nabla\chi\| \neq 0$  and the corresponding total area is

$$S_{acc} = \int \|\nabla\chi(\mathbf{r})\| \, d\mathbf{r} \quad (3)$$

In practice the gradient is computed numerically by a finite element method. Finally, the local unit vector normal to the surface, which is used to compute the density profiles is given by:

$$\mathbf{n} = \frac{\nabla\chi(\mathbf{r})}{\|\nabla\chi(\mathbf{r})\|} \quad (4)$$

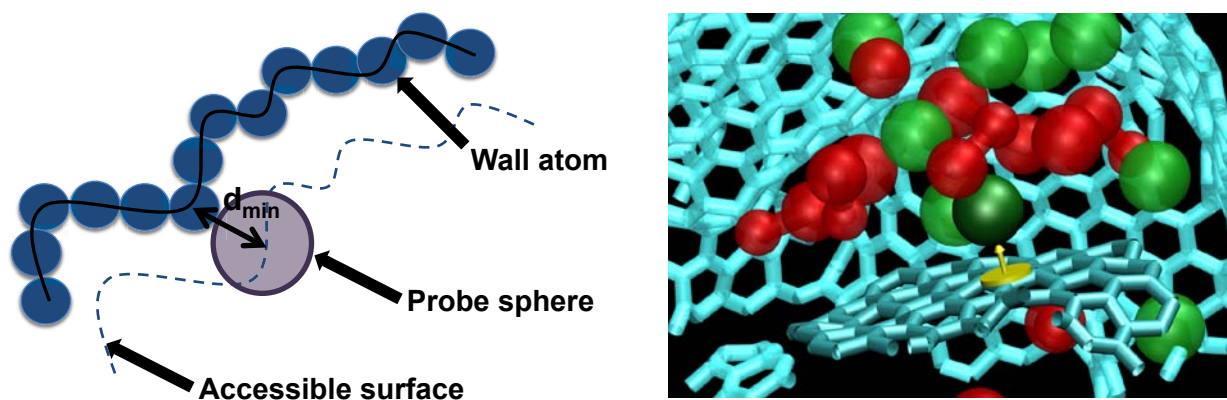


FIG. 3: The accessible surface area is determined as a function of the probe sphere. The results given in the main text correspond to argon as the probe sphere. The snapshot shows the local structure of the ionic liquid near a positive surface (+0.5 V) inside the CDC-1200. Blue: C-C bonds, red: BMI<sup>+</sup> and green: PF<sub>6</sub><sup>-</sup>. The ionic local densities are calculated with respect to the normal to the local surface (represented as a yellow arrow on the snapshot).

# Ionic density profiles

Density profiles calculated with respect to the normal to the local surface are given in the following figure. In the microporous materials, ions approach closer to the carbon surface whatever the applied potential. Despite an overall larger ionic density in graphite, the greater difference between cations and anions in CDCs demonstrates that the charge separation is more efficient in the latter case.

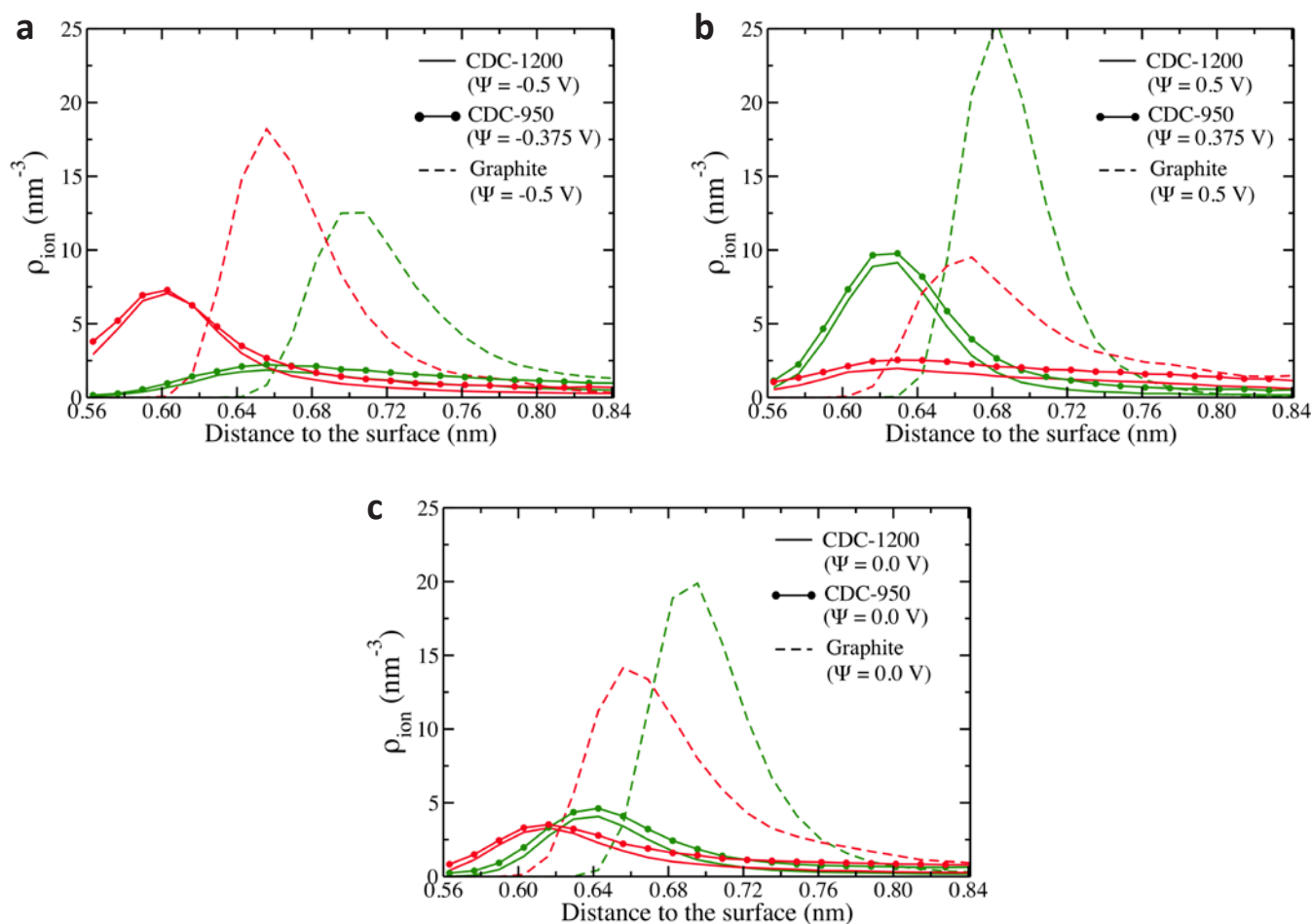


FIG. 4: Density profiles normal to the electrodes for all the materials studied in this work, for a negative potential (a), a positive potential (b), a zero potential (c). Green: PF<sub>6</sub><sup>-</sup> anions; red: BMI<sup>+</sup> cations.

### Accessible surface area and capacitance units

In the main text, integral capacitances are given in  $\text{F g}^{-1}$ , because these values are unambiguous in our setup as the number of carbon atoms is clearly known. On the contrary, for the microporous systems studied here, the normalized capacitance value (in  $\mu\text{F cm}^{-2}$ ) depends on the determined accessible surface area which is, as in experiments, a function of the probe size. Nevertheless, it is useful to have these normalized values for comparison. The values given in table II were obtained using the accessible surface areas calculated using the above method, these surface areas can differ from the experimental ones for two principal reasons: The probe size chosen may not represent exactly the actual size of argon and the value could be overestimated if closed volumes (not accessible experimentally) are taken into account. Results from literature are provided in table III for comparison. Experiments show that the capacitance is fairly constant<sup>2</sup> for the range of voltages that we study. The integral capacitance can therefore directly be compared to the experimentally measured differential capacitance. The value could be further refined by performing simulations for several voltages.

Material	Specific capacitance ( $\text{F g}^{-1}$ )	Normalized capacitance ( $\mu\text{F cm}^{-2}$ )
Graphite	30	2.15
CDC-1200	87	4.55
CDC-950	125	6.18

TABLE II: Specific and normalized capacitances for graphite and porous materials from this work.

Material and reference	Electrolyte	Specific capacitance (F g <sup>-1</sup> )	Normalized capacitance (μF cm <sup>-2</sup> )
Carbon nanotube <sup>3</sup>	[TEA][BF <sub>4</sub> ]-ACN (1M)	39	3.01
Carbon nanotube <sup>4</sup>	[EMI][BF <sub>4</sub> ]	6.5–9.75	0.5–1.5
Graphite <sup>5</sup>	[pyr <sub>13</sub> ][TFSI]	16.25–32.5	1.25–2.5
Metallic plates <sup>6</sup>	restricted primitive model	–	6–13

TABLE III: Specific and normalized capacitances from literature for various materials. When the capacitances were reported for positive and negative interfaces separately, we obtain the full cell value using  $\frac{1}{C_{tot}} = \frac{1}{C_+} + \frac{1}{C_-}$ . We obtain the specific capacitance from the normalized capacitance using the specific surface area of graphite (1300 m<sup>2</sup> g<sup>-1</sup>) except for the metallic plates which are not represented using an atomic description. The main difference between studies 3 and 4 lies in the choice of the porosities which are respectively the exterior and the interior of the carbon nanotube.

### Number of ions and occupied volumes

Number of ions	$\Psi < 0$	$\Psi = 0$	$\Psi > 0$	$N_+/N_- (\Psi < 0)$	$N_-/N_+ (\Psi > 0)$
CDC-1200	$N_+ = 104$	$N_+ = 82$	$N_+ = 66$	1.89	1.74
	$N_- = 55$	$N_- = 82$	$N_- = 115$		
CDC-950	$N_+ = 97$	$N_+ = 82$	$N_+ = 70$	1.90	1.69
	$N_- = 51$	$N_- = 82$	$N_- = 118$		

TABLE IV: Number of ions counted in the electrodes for different applied potentials and corresponding cations/anions ratios.

Occupied volume (Å <sup>3</sup> )	$\Psi < 0$	$\Psi = 0$	$\Psi > 0$
CDC-1200	16,762	15,837	16,070
CDC-950	15,613	15,837	16,775

TABLE V: Total volume occupied by anions and cations estimated using the van der Waals volumes of the ions.



**Other Supporting Online Material for this manuscript includes the following:**

**MovieS1:** Movie showing the degree of charging of the electrode atoms as a function of time (total time = 75 ps). Carbon atoms are coloured according to the charge  $q$  they carry (green:  $q < 0$ , red:  $q > 0$ , yellow:  $q \approx 0$ ), ions are not shown for clarity. This movie is extracted from a simulation with the CDC-1200 carbon and applying a potential difference of 1 V.

**MovieS2:** Movie showing the ions going into the electrodes (CDC-1200 carbon) during the first equilibration (total time of the movie = 150 ps). The carbon atoms are kept neutral during this simulation. Anions are coloured in green, cations in red and carbon atoms in light blue.

The movies were generated using the VMD software.<sup>7</sup>

- 
- <sup>1</sup> Palmer, J. C., Llobet, A., Yeon, S.-H., Fisher, J. E., Shi, Y., Gogotsi, Y., and Gubbins, K. E. Modeling the structural evolution of carbide-derived carbons using quenched molecular dynamics. *Carbon* **48**, 1116–1123 (2010).
  - <sup>2</sup> Chmiola, J., Largeot, C., Taberna, P.-L., Simon, P., and Gogotsi, Y. Desolvation of ions in subnanometer pores and its effect on capacitance and double-layer theory. *Angew. Chem., Int. Ed.* **47**, 3392–3395 (2008).
  - <sup>3</sup> Yang, L., Fishbine, B. H., Migliori, A., and Pratt, L. R. Molecular simulation of electric double-layer capacitors based on carbon nanotube forests. *J. Am. Chem. Soc.* **131**, 12373–12376 (2009).
  - <sup>4</sup> Shim, Y. and Kim, H. J. Nanoporous carbon supercapacitors in an ionic liquid: A computer simulation study. *ACS Nano* **4**, 2345–2355 (2010).
  - <sup>5</sup> Vatamanu, J., Borodin, O., and Smith, G. Molecular dynamics simulations of atomically flat and nanoporous electrodes with a molten salt electrolyte. *Phys. Chem. Chem. Phys.* **12**, 170–182 (2010).
  - <sup>6</sup> Kondrat, S., Georgi, N., Fedorov, M. V., and Kornyshev, A. A. A superionic state in nano-porous double-layer capacitors: insights from Monte Carlo simulations. *Phys. Chem. Chem. Phys.* **13**, 11359–11366 (2011).
  - <sup>7</sup> Humphrey, W., Dalke, A., and Schulten, K. VMD - Visual Molecular Dynamics. *J. Mol. Graphics* **14**, 33–38 (1996).